Arch. Mech., 50, 4, pp. 757–789, Warszawa 1998
FIFTY YEARS OF THE ARCHIVES OF MECHANICS

Plastic inclusion with moving boundary. Application to dislocation cell structures

X. LEMOINE, H. SABAR, M. BERVEILLER (METZ)
and J. MORREALE (FLORANGE)

BASED ON THE DETERMINATION of the Helmholtz free energy and the dissipation of an elastoplastic solid containing moving surfaces of plastic strain discontinuity, a micromechanical approach is developed to study the formation of dislocation cell structure and their effects on the mechanical behavior of metals. The results are applied to an evolutive two-phase microstructure representing the dislocation cell structure induced during plastic straining. The internal variables are reduced to the plastic strain of each mechanical phase, the volume fraction and the morphology of the ellipsoidal inclusion describing the cell structure. We obtain the conjugate forces according to the formalism of irreversible thermodynamics. Complementary relations describing the evolution of these internal variables are introduced in order to obtain the constitutive equation for the grain, the evolution of the microstructure as well as the hardening of the two phases. Preliminary results are presented and discussed in the case of a simplified situation.

1. Introduction

THE MODELLING of the elastoplastic behavior of metals and alloys from physical mechanisms (motion, storage and annihilation of dislocations) and the polycrystalline microstructure of the volume element (texture, grain boundaries) constitutes a difficult task requiring the introduction of different scales of description as well as scale transition methods. Classical meso-macro models (TAYLOR [1], SACHS [2], Self-consistent [3, 4]) taking into account the granular structure of the polycrystal, are based on the hypothesis of homogeneous multiple slip at the intragranular scale and a perfect intergranular interface (no debonding). Thus, using a self-consistent model formulated for large plastic strains [5, 6], the results obtained are by many aspects in good agreement with experiments, both for the overall behavior and the evolution of the internal state corresponding to texture, internal stresses and stored energy.

This description shows, however, its limits when applied to the description of the hardening during complex loading, studied experimentaly by HU and TEODOSIU [7]. It appears clearly that refining of the meso-macro transition has no sense except the case when the description of the intracrystalline behavior is improved to take into account the intragranular heterogeneization of the plastic deformation corresponding to the formation of dislocation cells.

The heterogeneity of the intragranular plastic strain field results from different mechanisms:

- the subdivision of a grain into zones with homogeneous single or multiple slip, related mainly to the discrete nature of the neighbouring grains [8];
- the formation of micro-shear bands corresponds to an intense localized shear [9, 10];
- the development of dislocation cells results from selforganization of the microstructure simultaneously due to the long range stress field, junction reactions between dislocations and mechanisms of annihilation related to the nature of the dislocations [11, 12].

The essential characteristics of the cellular structure may be summarized as follows:

- the formation of cells corresponds to a heterogeneous plastic strain field, weak inside walls and large in the cell interior;
- their topological and morphological aspects depend strongly on the macroscopic loading [13, 14];
- high dislocations density leads to a large hardening corresponding to a pronounced nonlocal effect, since plastic strain inside the cells increases the hardening in the walls where the dislocations are stored [15];
- finally, during sequential loading, the partial dissolution of the microstructure built during the first loading path is accompanied often by the formation of a new microstructure characteristic of the second loading path.

The current models describing the formation of dislocation cells can be cla ssified in three groups:

- Using numerical techniques based on cellular automatons [16, 18], discrete dislocations motion, multiplication and annihilation as well as storage can be described. Besides the huge memory and important CPU time required, these models are based on very specific boundary conditions and the dislocations move individually in a sequential manner so that collective behavior is absent.
- Considering plasticity described by the crystallographic slip mechanisms, AIFANTIS [19] and other authors have added a second gradient to the constitutive equation, to introduce a characteristic length and to reproduce the development of cells. Models using the concept of nonlocal hardening [20, 21] have also been introduced to describe the formation of cells and the intragranular plastic heterogeneization. The concept is indoubtedly correct, nevertheless it remains to ensure the validity of the introduced differential or integral operator which constitutes a difficult task.
- The first attempt for the description of dislocation cells, proposed by MUGHRABI and ESSMANN [11] is based on the representation of the cellular structure by a two-phase mechanical structure where the morphology of cells is a *priori* imposed, neglecting the effect of the external loading.

The aim of this paper is to formulate a model for the formation and evolution of the dislocation cells structure in the classical framework of crystal-plasticity (slip mechanism). In classical micromechanical description of the polycrystal, the discrete notion, interaction and storage of dislocations at grain boundaries are described using the slip rate as an average process variable. Continuity of displacement, velocity of particles and stress vector are required at grain boundaries. According to that, only (second order) long-range internal stresses are taken into account; pile ups at grain boundaries and discrete slip lines are neglected. One follows the same scheme of simplification for the intragranular heterogeneization corresponding to the formation of cell structures (Fig. 2). Dislocations are supposed to move inside the cells and walls and are stored in internal boundaries. It is worthwhile to notice that these walls are free surfaces, contrary to the grain boundaries, so that their morphological characteristics (shape, orientation) become new variables. Therefore, as in classical micromechanical plasticity, the plastification is still represented by slip rate inside the cells and the walls which are assumed to be moving boundaries. In such a way, one loses the precise description of the microstructure inside the walls but the (third order) long-range internal stresses are taken into account. For mobile boundaries, continuity of displacement and stress vector are always needed but the motion of the free surface allows some discontinuity in the particle velocity leading to a more complex problem.

In order to reduce the number of parameters describing the microstructure, one assumes that the cells may be considered as ellipsoidal inclusions with moving boundaries. This last assumption makes the model different from the previous one (Mughrabi) which assumes a fixed boundary.

In the second part, we determine the dissipation of an elastoplastic single crystal containing moving surfaces of plastic discontinuity from the evolution of the Helmholtz free energy and the power of external load. The results are applied in part 3 to an evolutive two-phase microstructure representing the dislocation cells structure inside the grain. In this way, the internal state and process variables reduce to the plastic strain of each phase, the volume fraction and the morphology of the ellipsoidal inclusion inside the grains of the polycrystal.

Complementary laws are introduced in order to obtain the constitutive equation for the grains, the evolution of the microstructure as well as the hardening of the two intragranular phases.

The transition from the grain level to the polycrystal is achieved by a classical elastoplastic self-consistent model described in [4, 5, 6].

Prelininary results are presented and discussed in the situation where the proportion of phases are treated as material parameters [13] and the concept of "Low Energy Dislocations Structures" (LEDS) [22, 23] is adopted to define the morphology of the microstructure.

2. Thermomechanical approach of mobile surface with plastic discontinuity

In this part the kinematical and thermodynamical aspects of a solid containing mobile surface discontinuities of plastic strain are developed. From the Helmholtz free energy, the intrinsic dissipation associated with the progress of the plastic deformation and the motion of surface discontinuities is given.

2.1. The kinematical description

Let us consider a solid with volume V bounded by an external surface ∂V. The reference configuration is assumed to be stress-free. The current configuration corresponds to V loaded by the displacement u^d on the boundary ∂V. We denote by $u(r)$ the total compatible displacement field of a point $r(x_1, x_2, x_3)$ from the reference configuration to the current one. The total distortion field $\beta(r)$ is given from the displacement gradient:

$$\beta(r) = \nabla \oplus u(r), \quad (\beta_{ij} = u_{i,j}) \,. \tag{2.1}$$

This total distortion results from:

- an elastic part $\beta^e(r)$, and
- a plastic part $\beta^p(r)$ with some discontinuity along surfaces S separating the volumes occupied by the plastic phases so that, in the small perturbation hypothesis, one obtains:

$$\beta(r) = \beta^e(r) + \beta^p(r). \tag{2.2}$$

Two fundamental tensors are derived from (2.1), the strain tensor being the symmetrical part of $\beta(r)$:

$$\varepsilon(r) = \frac{1}{2}(\beta(r) + {}^t\beta(r)) \tag{2.3}$$

and, the spin being its antisymmetrical part,

$$\omega(r) = \frac{1}{2}(\beta(r) - {}^t\beta(r)). \tag{2.4}$$

Combining (2.2), (2.3) and (2.4), the following expressions are obtained:

$$\begin{aligned} \beta(r) &= \varepsilon(r) + \omega(r), \\ \beta^e(r) &= \varepsilon^e(r) + \omega^e(r), \\ \beta^p(r) &= \varepsilon^p(r) + \omega^p(r) \,. \end{aligned} \tag{2.5}$$

When the solid is submitted to homogeneous distortion boundary conditions $u_i^d(r) = B_{ij}x_j$, the average B over V of the internal distorsion field β is given by

$$B = \frac{1}{V}\int_V \beta(r)dV = \frac{1}{V}\int_V (\beta^e(r) + \beta^p(r)dV. \tag{2.6}$$

For homogeneous elastic behavior, Eq. (2.6) leads to:

$$B = B^e + B^p, \tag{2.7}$$

where B^e and B^p are, respectively, the macroscopic elastic and plastic parts of the overall distorsion. They are defined by

$$\begin{aligned} B^e &= \frac{1}{V}\int_V \beta^e(r)dV, \\ B^p &= \frac{1}{V}\int_V \beta^p(r)dV. \end{aligned} \tag{2.8}$$

Decomposition (2.5) is also applied to macroscopic quantities:

$$\begin{aligned} B &= E + \Omega, \\ B^e &= E^e + \Omega^e, \\ B^p &= E^p + \Omega^p. \end{aligned} \tag{2.9}$$

The time evolution of B^p is related with an evolution of $\beta^p(r)$ and a motion of internal surfaces S.

The first step consists in taking the time derivative of $(2.8)_2$ where the local plastic distortion $\beta^p(r)$ is discontinuous across the surface S; S moves with time because the evolution of $\beta^p(r)$ is accompanied by a geometrical extension of the plastic phases. The time derivative of a volume integral containing a discontinuous integrand through a moving surface is given for instance in GERMAIN [24], and leads to

$$\dot{B}^p = \frac{d}{dt}\left[\frac{1}{V}\int_V \beta^p(r)dV\right] = \frac{1}{V}\int_V \dot{\beta}^p(r)dV - \frac{1}{V}\int_S [\beta^p(r)]w_\alpha n_\alpha dS. \tag{2.10}$$

In this equation $\dot{\beta}^p = \partial\beta^p/\partial t$ is the plastic distortion rate in all different plastic phases, $[\beta^p(r)] = \beta^{p+} - \beta^{p-}$ denotes the jump of $\beta^p(r)$ when crossing S, n_i is the unit normal to S taken from the negative to positive side, and w_α is the velocity of S (Fig. 1). $\dot{\beta}^p$ is the macroscopic plastic distortion rate, containing the evolution of the microstructure. It is difficult to get $\dot{\beta}^p$ for any distribution of

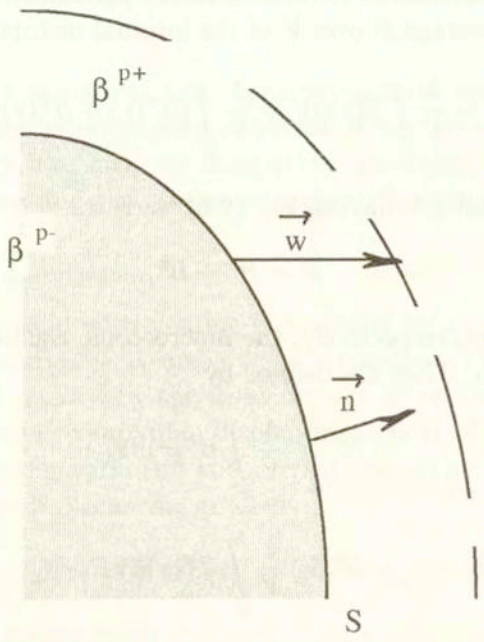

FIG. 1. Jump of plastic distorsion across a moving surface S.

plastic heterogeneity. To account for the cell dislocation structure, a two-phase approximation seems to be well adapted.

Case of a two-phase material

In this case, one assumes that the solid V consists of the assembly of two phases with respective volumes V^1 and V^2. The boundary between phases is given by mobile surface S. One notes that the unit normal n_i to S and the velocity w_α of S are directed into V^2.

If one assumes that the intra-phase heterogeneities are weak in comparison with the interphase one, $(2.8)_2$ becomes, for the two-phase material:

$$B^p = f\beta^{p_1} + (1-f)\beta^{p_2}, \tag{2.11}$$

where $f = V^1/V$ and $1 - f = V^2/V$ are, respectively, the volume fraction of phases 1 and 2. β^{p_1} and β^{p_2} are, respectively, the mean plastic distortions in V^1 and V^2 defined by:

$$\beta^{p_\alpha} = \frac{1}{V_\alpha}\int_{V\alpha} \beta^p(r)dV, \qquad (\alpha = 1, 2).$$

During the evolution, two contributions can be distinguished in (2.10):

• The first one corresponds to the volumic variation of plastic distortion and is written in this case:

$$\frac{1}{V}\int_V \dot{\beta}(r)dV = f\dot{\beta}^{p_1} + (1-f)\dot{\beta}^{p_2}.$$

• The second one is the contribution due to the motion of surface S. Assuming that $[\beta^p(r)]$ is uniform over the surface S and equal to $\beta^{p_2} - \beta^{p_1}$ and taking into account the obvious relation $\dot{f} = \frac{1}{V}\int_S w_\alpha n_\alpha dS$, one obtains

$$\frac{1}{V}\int_S [\beta^p(r)] w_\alpha n_\alpha dS = [\beta^p]\dot{f}.$$

With these expressions, (2.10) is reduced to

$$\dot{B}^p = f\dot{\beta}^{p_1} + (1-f)\dot{\beta}^{p_2} - [\beta^p]\dot{f}. \tag{2.12}$$

Equations (2.10) and (2.12) indicate the nature of internal variables describing the inelastic behavior of the solid:

• plastic flow in the two phases,

• the motion of surface between these phases or the evolution of the voluminal fraction f.

The evolution of these internal variables are deduced from a thermodynamic analysis giving the thermodynamical forces in the internal variables.

2.2. The thermomechanical description

The evolution of a thermodynamical system with irreversible processes is derived generally from the maximal dissipation principe [25, 26]. In the case of quasi-static and isothermal approximation, the dissipation is given by the difference between the external power and the variation of the Helmholtz free energy.

In the following, one calculates successively the free energy, its time derivative, the external power and the intrinsic dissipation for a solid containing mobile discontinuity surfaces.

2.2.1. Helmholtz free energy. In case of isothermal approximation, the Helmholtz free energy density reduces to elastic energy:

$$w(r) = \frac{1}{2}\sigma(r) : \varepsilon^e(r).$$

For a volume V, we have:

$$W = \int_V w(r)dV. \tag{2.13}$$

The stress tensor $\sigma(r)$ and elastic strain $\varepsilon^e(r)$ are related by the usual constitutive relations:

$$\sigma(r) = C : \varepsilon^e(r), \tag{2.14}$$

where the homogeneous elastic moduli C exhibit the usual symmetries:

$$C_{ijkl} = C_{jikl} = C_{ijlk} = C_{klij}. \tag{2.15}$$

Using (2.2), (2.3) and (2.5)

$$\varepsilon(r) = \varepsilon^e(r) + \varepsilon^p(r), \tag{2.16}$$

the Helmholtz free energy (2.13) is written as

$$W = \frac{1}{2}\int_V \sigma(r) : (\varepsilon(r) - \varepsilon^p(r))\, dV. \tag{2.17}$$

2.2.2. Evolution of the Helmholtz free energy. For a load variation, the evolution of the Helmholtz free energy results from the progress of plastic strain $\varepsilon^p(r)$ and the propagation of discontinuity surface S. The jump of $\varepsilon^p(r)$ across S implies the discontinuities of $\varepsilon(r)$, $\sigma(r)$ and $w(r)$. By time differentiation of (2.13), the evolution of Helmholtz free energy of the system is given by

$$\dot{W} = \int_V \dot{w}(r)dV - \int_S [w(r)]w_\alpha n_\alpha dS. \tag{2.18}$$

Due to the symmetry of C and using (2.14) and (2.16), the first integral is transformed into

$$\int_V \dot{w}(r)dV = \int_V \sigma(r) : (\dot{\varepsilon}(r) - \dot{\varepsilon}^p(r))dV. \tag{2.19}$$

Assuming uniform elasticity, $[w]$ is expressed by

$$[w] = \frac{1}{2}\left\{\sigma^+(r) : (\varepsilon^+(r) - \varepsilon^{p+}(r)) - \sigma^-(r) : (\varepsilon^-(r) - \varepsilon^{p-}(r))\right\} \tag{2.20}$$

or

$$[w] = \frac{1}{2}\left\{\sigma^+(r) + \sigma^-(r)\right\} : [\varepsilon(r) - \varepsilon^p(r)]. \tag{2.21}$$

From (2.19) and (2.21), (2.18) is given by

$$\dot{W} = \int_V \sigma(r) : (\dot{\varepsilon}(r) - \dot{\varepsilon}^p(r))dV - \frac{1}{2}\int_S \left\{\sigma^+(r) + \sigma^-(r)\right\} : [\varepsilon(r) - \varepsilon^p(r)]w_\alpha n_\alpha dS\,. \tag{2.22}$$

2.2.3. External power. The power $\mathcal{P}_{\text{ext}}$ developed by the forces $T_i = \sigma_{ij} n_j$ applied to the external surface S^{ex} of volume V associated with the particle velocity $v_i (= \dot{u}_i)$ is defined by

$$\mathcal{P}_{\text{est}} = \int_{S^{\text{ex}}} T_i v_i dS^{\text{ex}} = \int_{S^{\text{ex}}} \sigma_{ij} n_j v_i dS^{\text{ex}}. \tag{2.23}$$

Using the divergence theorem, when the volume V contains a discontinuity surface S, the surface integral (2.23) is transformed to a volume integral:

$$\mathcal{P}_{\text{ext}} = \int_V (\sigma_{ij} v_i)_{,j} \, dV + \int_S [\sigma_{ij} n_j v_i] dS. \tag{2.24}$$

The conditions of continuity of the displacement and the interfacial traction across S yield

$$[u_i] = 0 \tag{2.25}$$

and

$$[\sigma_{ij} n_j] = 0. \tag{2.26}$$

During the propagation of the surface S, these conditions hold at any time t. Thus the jump in the components of material velocity v_i is determined by taking the time derivative of (2.25). One gets the compatibility equation of HADAMARD [27]:

$$[v_i] = -[u_{i,j}] n_j w_\alpha n_\alpha. \tag{2.27}$$

From (2.25) and (2.26) and the equilibrium equation, in the absence of volumic forces ($\sigma_{ij,j} = 0$), the power $\mathcal{P}_{\text{ext}}$ becomes:

$$\mathcal{P}_{\text{ext}} = \int_V \sigma_{ij} v_{i,j} dV - \int_S \sigma_{ij} n_j [u_{i,k}] n_k w_\alpha n_\alpha dS. \tag{2.28}$$

The continuity of displacement along the surface S imposes the relation on the jump of displacement gradient:

$$[u_{i,j}] = \lambda_i n_j, \tag{2.29}$$

where λ is an arbitrary vector function of position.

The term $\sigma_{ij} n_j [u_{i,k}] n_k$ is also equal to $\sigma_{ij} [u_{i,j}]$ from compatibility conditions (2.25) and (2.26) along the surface S, so that

$$\sigma_{ij} n_j [u_{i,k}] n_k = \sigma_{ij} [\varepsilon_{ij}] = \frac{1}{2} \left\{ \sigma_{ij}^+ + \sigma_{ij}^- \right\} [\varepsilon_{ij}]. \tag{2.30}$$

Using (2.30), the external power is written as

$$\mathcal{P}_{\text{ext}} = \int_V \sigma(r) : \dot{\varepsilon}(r) dV - \frac{1}{2} \int_S \{\sigma^+(r) + \sigma^-(r)\} : [\varepsilon(r)] w_\alpha n_\alpha dS. \tag{2.31}$$

2.2.4. Analysis of the intrinsic dissipation. During the evolution of the system, the intrinsic dissipation is given by

$$\mathcal{D} = \mathcal{P}_{\text{ext}} - \dot{W}. \tag{2.32}$$

Using (2.22) and (2.31), the intrinsic dissipation is finally given by

$$\mathcal{D} = \int_V \sigma(r) : \dot{\varepsilon}^p(r) dV - \frac{1}{2} \int_S \{\sigma^+(r) + \sigma^-(r)\} : [\varepsilon^p(r)] w_\alpha n_\alpha dS. \tag{2.33}$$

The first term in (2.33) is the volume dissipation due to the evolution of plastic strain. The second one is due to the propagation of surface between the phases.

Two quantities appear: the energy release rate $-\frac{1}{2}\{\sigma^+(r) + \sigma^-(r)\} : [\varepsilon^p(r)]$ which corresponds to the thermodynamic force associated with the normal velocity $w_\alpha n_\alpha$ of the surface S, and the thermodynamic force σ associated with the plastic strain rate $\dot{\varepsilon}^p(r)$.

For any microstructure, the determination of the intrinsic dissipation is difficult because the variables describing this internal structure are complex. In the next section, an application of this approach is developed in the case of a two-phase material with ellipsoidal microstructure.

3. Two phase model for a crystal with evolution of microstructure

3.1. Representation of the intragranular microstructure

During plastic strain of a metal, dislocation cells are formed leading to high dislocation density gradients which allows us to describe the cell structure as a two-phase composite, the cell interiors (zones with a low dislocation density) and the walls (zones with a high dislocation density) represented, respectively, by soft (s) and hard (h) phases. This partition of the volume V of a grain into two domains V^s (s = soft) and V^h (h = hard) implies for a macroscopic variable M described as a voluminal average of the corresponding local variable m in V,

$$M = \frac{1}{V} \int_V m(r) dV \tag{3.1}$$

which can be simplified by

$$M = f m^s + (1 - f) m^h, \tag{3.2}$$

where $f = V^s/V$ and $1 - f = V^h/V$ are respectively the volume fraction of soft and hard phases. The average values m^s and m^h are defined by

$$m^\alpha = \frac{1}{V^\alpha} \int_{V^\alpha} m(r)dV, \qquad (\alpha = h, s). \tag{3.3}$$

TEM results show that the dislocation cell shape may be approximated by ellipsoids [13, 28]. This allows us to consider only an averaged description of the cell structure where the cell shape is an ellipsoid with semi-axes $a_i (i = 1, 2, 3)$ and Euler angles $\alpha_i (i = 1, 2, 3)$ describing the orientation of the ellipsoid principal reference frame versus the crystalline lattice. On the other hand, the cell with its dislocation wall is described as a coated inclusion. Thus, the cell is represented by two similar and concentric ellipsoids.

The topology of the coated inclusion problem assumes that an inclusion (interior cell) with plastic strain ε^{P_s} and volume V^s is surrounded by a thin coating of the second phase (wall) with plastic strain ε^{P_h} and volume V^h. The coating is bounded at its outer boundary by a surrounding homogenous material (matrix) whose plastic strain is E^P (Fig. 2). V^e denotes the volume of the composite inclusion (inclusion + coating). If N is the number of cells inside V, one has

$$V = Nv^e = N(v^h + v^s). \tag{3.4}$$

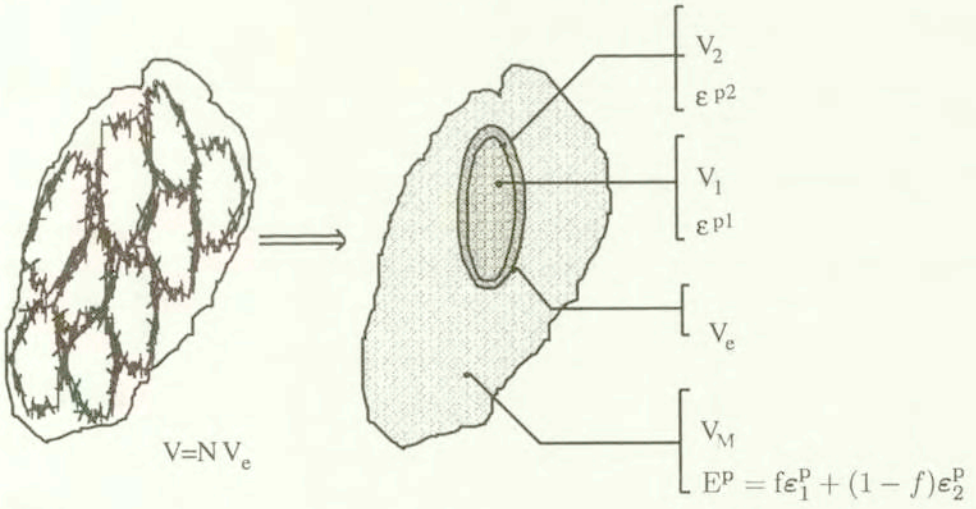

FIG. 2. Simplified representation of the microstructure of dislocation cells by a two-phase material with coated inclusions.

The proportion of the phase h in the grain is supposed to be the same as in the composite inclusion. Thus, the volume fraction of the two phases are given by

$$f = \frac{Nv^s}{V} = \frac{V^S}{V} = \frac{v^S}{v^e}, \tag{3.5}$$

$$1 - f = \frac{Nv^h}{V} = \frac{V^h}{V} = \frac{v^h}{v^e} \,. \tag{3.6}$$

An Eshelby-Kröner-type approximation is used to account for the interactions between the coated inclusions. This approximation assumes that each coated inclusion is embedded in an infinitely extended medium (matrix) having macroscopic plastic strain E^P equal to volume average of the local plastic strain $\varepsilon^p(r)$ on V.

This representation implies that there is no creation of new composite inclusion during the evolution of the system: $\dot{N} = 0$. Thus, with (3.4) and $\dot{V} = 0$ one gets

$$\dot{v}^e = 0. \tag{3.7}$$

Finally, the internal variables describing the microstructure of the grain and the field $\varepsilon^p(r)$ are:

- the plastic strain ε^{P_s} inside the cells,
- the plastic strain ε^{P_h} inside the walls,
- the volume fraction f of cells,
- the morphology of the internal inclusion a_p and α_p described by a tensor $A(a_p, \alpha_p)$ defined by

$$A_{ij} x_i x_j = 1. \tag{3.8}$$

The components A_{ij} can be deduced from the variables a_p and α_p (see Appendix B).

3.2. Calculation of the dissipation

For the simplified representation (Fig. 2) of the microstructure, the dissipation $\mathcal{D}$ resulting from the plastic strain rate $\dot{\varepsilon}^p(r)$ and the motion $w_\alpha n_\alpha$ of surfaces S^1 and S^e surrounding, respectively, v^1 and v^e is calculated. From (2.33), this dissipation is expressed by

$$\mathcal{D} = \int_v \sigma(r) : \dot{\varepsilon}^p(r) dV - \frac{N}{2} \int_{S^1} \left\{ \sigma^{+1}(r) + \sigma^{-1}(r) \right\} : [\varepsilon^p(r)]^1 w_\alpha^1 n_\alpha^1 dS^1 \tag{3.9}$$

$$- \frac{N}{2} \int_{S^e} \left\{ \sigma^{+e}(r) + \sigma^{-e}(r) \right\} : [\varepsilon^p(r)]^e w_\alpha^e n_\alpha^e dS^e$$

or $\mathcal{D} = \mathcal{D}^1 + \mathcal{D}^2 + \mathcal{D}^3$ where $[\varepsilon^p(r)]^e$ and $[\varepsilon^p(r)]^1$ are respectively, the jumps of plastic strain across S^e and S^1. In case of two phases, the plastic strain rate is given by

$$\begin{aligned} \dot{\varepsilon}^p(r) &= \dot{\varepsilon}^{p_s}, \quad r \in V^s, \\ \dot{\varepsilon}^p(r) &= \dot{\varepsilon}^{p_h}, \quad r \in V^h. \end{aligned} \tag{3.10}$$

Consequently, it is possible to evaluate the first integral $\mathcal{D}^1$ in (3.9):

$$\mathcal{D}^1 = N\sigma^s : \dot{\varepsilon}^{p_s} v^s + N v^h \sigma^h : \dot{\varepsilon}^{p_h}, \tag{3.11}$$

where σ^s and σ^h are the mean stress in each phase defined by (3.3).
For the evaluation of the surface integrals in (3.9), an enlargement of the zones near the surfaces S^1 and S^e allows us to determine the interfacial stresses (Fig. 3).

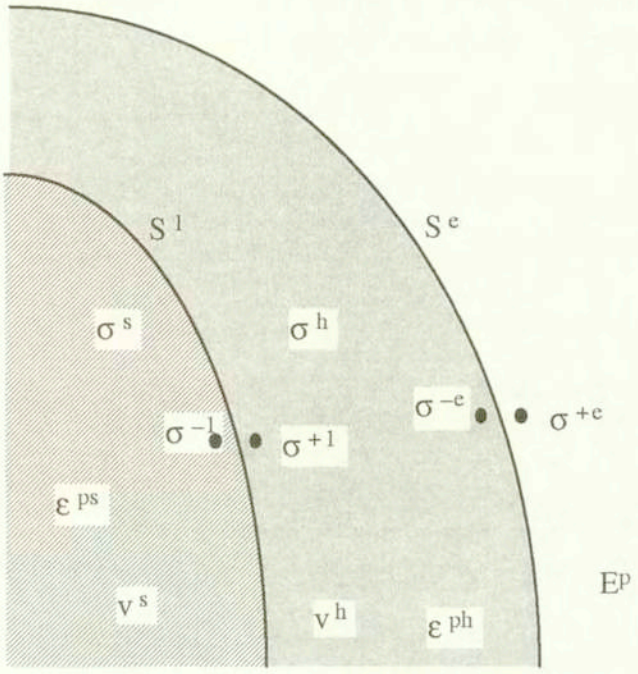

FIG. 3. Definition of stresses near surface S^1 and S^e.

In the second surface integral $\mathcal{D}^2$ in (3.9), the stress σ^{-1} inside the ellipsoid v^1 is uniform and equal to σ^s . This stress is obtained through the Eshelby-Kröner formula [30, 31], namely

$$\sigma^s = \Sigma - (1-f)C : (I - S^E) : \Delta\varepsilon^P, \tag{3.12}$$

where Σ is the macroscopic stress given by (3.1), S^E is the Eshelby tensor for the inclusion v^1 (see Appendix B), I is the fourth order unit tensor, and $\Delta\varepsilon^p = \varepsilon^{p_s} - \varepsilon^{p_h}$. The stress σ^h is deduced from (3.3) and given by

$$\sigma^h = \Sigma + fC : (I - S^E) : \Delta\varepsilon^P. \tag{3.13}$$

Using the interfacial operators [29], the stress σ^{+1} is linked to the stress σ^{-1} by

$$\sigma^{+1} = \sigma^{-1} - Q^1 : [\varepsilon^p]^1 \tag{3.14}$$

with $[\varepsilon^p]^1 = \varepsilon^{p_h} - \varepsilon^{p_s} = -\Delta\varepsilon^p$ and the interfacial operator Q^1 is defined in Appendix A. Due to (3.12) and (3.14), the second surface integral $\mathcal{D}^2$ in (3.9) becomes

$$\mathcal{D}^2 = \frac{N}{2}\sigma^s : \Delta\varepsilon^p \int_{S^1} w_\alpha^1 n_\alpha^1 dS^1 + \frac{N}{2}\Delta\varepsilon^p : \int_{S^1} Q^1 w_\alpha^1 n_\alpha^1 dS^1 : \Delta\varepsilon^p. \tag{3.15}$$

The first surface integral in (3.15) describes the evolution of the volume v^1 bounded by S^1. The solution of the integral J defined by

$$J^1 = \int_{S^1} Q^1 w_\alpha^1 n_\alpha^1 dS^1$$

is given in Appendix A,

$$J^1 = C : (I - S^E)\dot{v}^1 + C : (S^2 : \dot{A})v^1, \tag{3.16}$$

and (3.15) is reduced to

$$\mathcal{D}^2 = N\sigma^S : \Delta\varepsilon^p \dot{v}^S + \frac{N}{2}\Delta\varepsilon^p : C : (I - S^E) : \Delta\varepsilon^p \dot{v}^S + \frac{N}{2}\Delta\varepsilon^p : C : (S^2 : \dot{A}) : \Delta\varepsilon^p v^S \tag{3.17}$$

where $S^2 = \partial S^E / \partial A$ (see Appendix B).

A similar step for the evaluation of the surface integral $\mathcal{D}^3$ in (3.9) leads to

$$\mathcal{D}^3 = -\frac{N}{2}\int_{S^e} \{\sigma^{+e}(r) + \sigma^{-e}(r)\} : [\varepsilon^p(r)]^e w_\alpha^e n_\alpha^e dS^e, \tag{3.18}$$

where $\sigma^{+e} = \sigma^{-e} - Q^e : [\varepsilon^p]^e$ and $[\varepsilon^p]^e = E^P - \varepsilon^{ph} = f\Delta\varepsilon^p$.

Since $[\varepsilon^p]^e$ is assumed to be uniform along S^e, $\mathcal{D}^3$ is given by

$$D^3 = -Nf\Delta\varepsilon^p : \int_{S^e} \sigma^{-e} w_\alpha^e n_\alpha^e dS^e + \frac{Nf^2}{2}\Delta\varepsilon^p : \int_{S^e} Q^e w_\alpha^e n_\alpha^e dS^e : \Delta\varepsilon^p. \tag{3.19}$$

Contrary to the relation (3.12), σ^{-e} is not uniform along S^e. A time derivative of the mean value σ^h over the volume v^h allows us to account for the first surface integral I in (3.19). Indeed, the volume integral defining σ^h is

$$v^h\sigma^h = \int_{v^h} \sigma(r)dV. \tag{3.20}$$

The volume v^h is bounded by the surfaces S^1 and S^e and the stress in v^h is equal to σ^{+1} and σ^{-e}, respectively, near S^1 and S^e.

During the evolution of v^h, one has

$$\frac{d}{dt}(v^h\sigma^h) = \int_{v^h} \dot{\sigma}(r)dV + \int_{S^e} \sigma^{-e}(r)w_\alpha^e n_\alpha^e dS^e - \int_{S^1} \sigma^{+1}(r)w_\alpha^1 n_\alpha^1 dS^1. \tag{3.21}$$

The first term in (3.21) is

$$\frac{d}{dt}(v^h\sigma^h) = \dot{v}^h\sigma^h + v^h\dot{\sigma}^h. \tag{3.22}$$

From (3.21) and (3.22), the surface integral I in (3.19) is equal to

$$I = \int_{S^e} \sigma^{-e}(r)w_\alpha^e n_\alpha^e dS^e = \dot{v}^h\sigma^h + \int_{S^1} \sigma^{+1}(r)w_\alpha^1 n_\alpha^1 dS^1. \tag{3.23}$$

According to (3.22), (3.23) and (3.16), I is written as

$$I = \sigma^h\dot{v}^h + C : (I - S^E) : \Delta\varepsilon^p\dot{v}^s + C : (S^2 : \dot{A}) : \Delta\varepsilon^p v^s. \tag{3.24}$$

Due to (3.4) to (3.7) and using the expressions (3.12) and (3.13), I reduces to

$$I = C : (S^2 : \dot{A}) : \Delta\varepsilon^p v^s. \tag{3.25}$$

The calculation of the second surface integral J^2 in (3.19) is identical to the surface integral J^2 in (3.15) if S^1 and v^1 are replaced, respectively, by S^e and v^e. In the case of homothetic coated inclusions, the Eshelby tensors corresponding to the ellipsoids v^1 and v^e are equal. Thus, with the condition (3.7), J^2 is given by

$$J^2 = \int_{S^e} Q^e w_\alpha^e n_\alpha^e dS^e = C : (S^2 : \dot{A})v^e. \tag{3.26}$$

With these results, (3.19) becomes:

$$D^3 = -Nf\Delta\varepsilon^p : C : (S^2 : \dot{A}) : \Delta\varepsilon^p v^s + \frac{1}{2}Nf^2\Delta\varepsilon^p : C(S^2 : \dot{A}) : \Delta\varepsilon^p v^e. \tag{3.27}$$

Finally, with (3.4) to (3.6) and the solutions of the integrals $\mathcal{D}^1$, $\mathcal{D}^2$ and $\mathcal{D}^3$, the dissipation $\mathcal{D}$ per unit volume is expressed by

$$\frac{\mathcal{D}}{V} = f\sigma^s : \dot{\varepsilon}^{p_s} + (1-f)\sigma^h : \dot{\varepsilon}^{p_h} + \frac{1}{2}f(1-f)\Delta\varepsilon^p : C : (S^2 : \dot{A}) : \Delta\varepsilon^p \tag{3.28}$$

$$+\dot{f}\left\{\sum : \Delta\varepsilon^p - \frac{1}{2}(1-2f)\Delta\varepsilon^p : C : (I - S^E) : \Delta\varepsilon^p\right\}.$$

Generally the dissipation is expressed in the following manner:

$$\frac{\mathcal{D}}{V} = F_i(\Sigma, X)\dot{X}_i \tag{3.29}$$

where X_i are the internal variables of the thermodynamical system, and F_i are the thermodynamical forces acting on X_i. Here, the thermodynamical forces associated with the internal variables $\varepsilon^{p_s}, \varepsilon^{p_h}$, f and A are given by:

$$\begin{aligned} F_{\varepsilon^{Ps}} &= \sigma^S, \\ F_{\varepsilon^{Ph}} &= \sigma^h, \\ F_f &= \Sigma : \Delta\varepsilon^p - \frac{1}{2}(1-2f)\Delta\varepsilon^p : C : (I - S^E) : \Delta\varepsilon^p, \\ F_A &= \frac{1}{2}f(1-f)\Delta\varepsilon^p : C : S^2 : \Delta\varepsilon^p. \end{aligned} \tag{3.30}$$

Contrary to the kinematical analysis (Sec. 2.1) where the internal variables are reduced to $\varepsilon^{P_s}, \varepsilon^{p_s}$ and f, the analysis of the dissipation shows an additionnal internal variable corresponding to the morphology (shape and orientation) of the cell structure described by A.

To complete the study, complementary equations describing the evolution of these internal variables have to be introduced.

3.3. Complementary relations and global behavior

The analysis developed in Secs. 2 and 3 allows us to relate internal variables describing possible evolution of the microstructure with the mechanical state. In the case of reversible processes, the thermodynamical forces have to be taken equal to zero. This provides additional equations for the internal variables. For thermodynamical irreversible processes like in the classical plasticity approach, critical forces $F_i^c(X)$ are introduced. In this case the evolution $\dot{X}_i$ of internal variables X_i is given by

$$\begin{aligned} \dot{X}_i = 0 \quad \text{if} \quad & \begin{cases} F_i(\Sigma, X) < F_i^c(X), \\ \forall \dot{F}_i(\Sigma, X); \end{cases} \\ \dot{X}_i = 0 \quad \text{if} \quad & \begin{cases} F_i(\Sigma, X) = F_i^c(X), \\ \dot{F}_i(\Sigma, X) \leq \dot{F}_i^c(X); \end{cases} \\ \dot{X}_i \neq 0 \quad \text{if} \quad & \begin{cases} F_i(\Sigma, X) = F_i^c(X), \\ \dot{F}_i(\Sigma, X) = \dot{F}_i^c(X). \end{cases} \end{aligned} \tag{3.31}$$

Using the consistency rule,

$$\dot{F}_i(\Sigma, X) = \dot{F}_i^c(X) \,, \tag{3.32}$$

the following system with unknows $\dot{X}_i$

$$\left(\frac{\partial F_i^c}{\partial X_j}(X) - \frac{\partial F_i}{\partial X_j}(\Sigma, X)\right)\dot{X}_j = \frac{\partial F_i}{\partial \Sigma}(\Sigma, X) : \dot{\Sigma} \tag{3.33}$$

or, formally

$$\dot{X} = K : \dot{\Sigma} \,, \tag{3.34}$$

gives the evolution of the internal variables as a function of the loading parameter $\dot{\Sigma}$.

From

$$\dot{\Sigma} = C : (\dot{E} - \dot{E}^p) \tag{3.35}$$

and

$$\dot{E}^p = f\dot{\varepsilon}^p + (1-f)\dot{\varepsilon}^{p_h} + \dot{f}\Delta\varepsilon^p \tag{3.36}$$

or, formally

$$\dot{E}^p = M \cdot \dot{X} \,, \tag{3.37}$$

we have for a given $\dot{E}$:

$$\dot{X} = (I + K : C : M)^{-1} : K : C : \dot{E}$$

and

$$\dot{E}^p = M : (I + K : C : M)^{-1} : K : C : \dot{E}.$$

So, the overall behavior of the grain is written as:

$$\dot{\Sigma} = L : \dot{E}, \tag{3.38}$$

where L is the instantaneous elastoplastic modulus of the grain given by

$$L = C : (I - M : (I + K : C : M)^{-1} : K : C). \tag{3.39}$$

In the case of crystalline metals, dislocations are restricted to move on the crystallographic slip systems. As a first approximation, the walls are considered

as a crystallographic part of the grain, in spite of their high defect density. Furthermore the slip planes are assumed to remain continuous through the walls. Thus the plastic glide γ is introduced such as

$$\dot{\varepsilon}_{ij}^{p_\alpha} = R_{ij}^g \dot{\gamma}_\alpha^g, \qquad (\alpha = s, h), \tag{3.40}$$

where the Schmid tensor R_{ij}^g for the system g is given by

$$R_{ij}^g = \frac{1}{2}(m_i^g n_j^g + m_j^g n_i^g). \tag{3.41}$$

n_i is the unit normal to the slip plane and m_i is the slip direction. In order to obtain the tangent moduli (3.39), the critical forces $F_i^c(X)$ are introduced.

In case of time-independent plasticity, the evolution of these critical forces as a function of internal variables X_i is generally given by:

$$\dot{F}_i^c = \mathcal{H}^{ij} \dot{X}_j; \tag{3.42}$$

$\mathcal{H}^{ij} = \partial F_i^c / \partial X_j$ is the interaction matrix between the different internal variables X_i. According to different types of internal variables, (3.42) is explicitly written in the form

$$\begin{pmatrix} \dot{F}^c_{\gamma_S^i} \\ \dot{F}^c_{\gamma_h^i} \\ \dot{F}^c_f \\ \dot{F}^c_{a_i} \\ \dot{F}^c_{\alpha_i} \end{pmatrix} = \begin{pmatrix} \mathcal{H}^{ij}_{ss} & \mathcal{H}^{ij}_{hs} & \mathcal{H}^{ij}_{sf} & \mathcal{H}^{ij}_{sa} & \mathcal{H}^{ij}_{s\alpha} \\ \mathcal{H}^{ij}_{hs} & \mathcal{H}^{ij}_{hh} & \mathcal{H}^{ij}_{hf} & \mathcal{H}^{ij}_{ha} & \mathcal{H}^{ij}_{h\alpha} \\ \mathcal{H}^{ij}_{fs} & \mathcal{H}^{ij}_{fh} & \mathcal{H}^{ij}_{ff} & \mathcal{H}^{ij}_{fa} & \mathcal{H}^{ij}_{f\alpha} \\ \mathcal{H}^{ij}_{as} & \mathcal{H}^{ij}_{ah} & \mathcal{H}^{ij}_{af} & \mathcal{H}^{ij}_{aa} & \mathcal{H}^{ij}_{a\alpha} \\ \mathcal{H}^{ij}_{\alpha s} & \mathcal{H}^{ij}_{\alpha h} & \mathcal{H}^{ij}_{\alpha f} & \mathcal{H}^{ij}_{\alpha a} & \mathcal{H}^{ij}_{\alpha\alpha} \end{pmatrix} \begin{pmatrix} \dot{\gamma}_s^j \\ \dot{\gamma}_h^j \\ \dot{f} \\ \dot{a}_j \\ \dot{\alpha}_j \end{pmatrix}. \tag{3.43}$$

The submatrices $\begin{pmatrix} \mathcal{H}_{ss} & \mathcal{H}_{sh} \\ \mathcal{H}_{hs} & \mathcal{H}_{hh} \end{pmatrix}$ correspond to the hardening matrices between slip γ of each phase. One finds here the selfhardening, in other words the hardening of a slip system on itself, and the latent hardening defined by the hardening of a system by an other active slip system. The terms $\mathcal{H}_{sh}$ and $\mathcal{H}_{hs}$ determine the hardening of a phase by the other ones (non-local hardening). The components of this submatrix are obtained from dislocation concepts like creation or annihilation [11, 32, 33]:

$$\begin{aligned} H_{hs}^{gh} &= \frac{(1-f)b\mu^2}{\tau_{ch}^g - \tau_{ch}^{0g}} \left(\frac{a_{(g)h}}{L^{(h)}} - y a_{(g)l} \rho_h^l A_{hs}^{(l)h} \right), \quad H_{sh}^{gh} = 0, \\ H_{hh}^{gh} &= -\frac{(1-f)b\mu^2}{\tau_{ch}^g - \tau_{ch}^{0g}} y a_{(g)l} \rho_H^l A_{hh}^{(l)h}, \quad H_{ss}^{gh} = \frac{f \alpha_{ss}}{\tau_{cs}^g - \tau_{cs}^{0g}} a_{(g)h}, \end{aligned} \tag{3.44}$$

where b is the modulus of the Burgers vector, μ the elastic shear modulus, L^g the mean free path of dislocations in cell interiors, y a dislocation annihilation distance, ρ_α^l the dislocation density, $\tau_{c\alpha}^{0g}$ the initial critical shear stress and $a_{(g)h}$ denotes the anisotropy of the dislocation interactions [34].

4. Applications

Despite the fact that interaction matrix $\mathcal{H}^{ij}$ remains partially unknown, some first conclusions can be derived from the micromechanical approach developed in this paper. Numerical applications can be obtained using some additional assumptions. These assumptions reduce the field of validity of the developed model but are consistent with the physical aspects considered. In Secs. 2 and 3, the elastoplastic behavior of the grains was established. For the meso-macro scales transition (from the grains to the polycrystal), a classical elastoplastic self-consistent scheme is used so that the effects of fixed grain boundaries are taken into account (interactions of grains with the surrounding homogenous material). This model is extensively presented and discussed in [3 – 6]. The numerical application is restricted to a uniaxial tensile test.

4.1. Simplifying hypotheses

The analysis of dislocation in cell structures induced during a monotoneous path allows us to assume that the volume fraction f remains practically constant during plastic straining [13]. Therefore one assumes that the volume fraction of cells is no longer an internal variable but becomes a material parameter, so that $\dot{f} = 0$. The concept of Low Energy Dislocation Structure (LEDS) popular in physical metallurgy [22 – 23] allows to assume that the microstructure morphology adapts itself instantaneously to the loading. This second simplifying assumption corresponds to an organisation of cell structure which minimizes the free energy with respect to the corresponding variables. The consequence of this hypothesis gives

$$F_A = 0 \quad \text{and} \quad \dot{F}_A = 0$$

and by (3.37), the thermodynamical force F_A is equal to zero, so that

$$F_A = \frac{1}{2} f(1-f)\Delta\gamma R : C : S^2 : R\Delta\gamma = 0. \tag{4.1}$$

The time derivative of (4.1) gives the evolution of the parameters of the ellipsoid and is a function of the slip rates $\dot{\gamma}$.

4.2. Input data used for the calculation

The calculations are performed for a BCC polycrystal without initial texture (100 grains). Isotropic and homogeneous elasticity ($\mu = 80$ GPa, $\nu = 0.3$) and

slip systems of type $\{110\} < 111 >$ are assumed. The initial critical shear stress is assumed to be identical for all the systems of each phase and equal to 65 MPa. Characteristics of dislocations are: $b = 2.5$ Å, $L = 6.4$ μm, $a = 1.5$ Å, $y = 4.7$, $\alpha_{ss} = 900$ (MPa)^2. Finally the ellipsoid describing the cell shape in each grain is initially nearly spherical: $a_1 = 1$, $a_2 = 1.02$, $a_3 = 0.98$.

4.3. Numerical results

Figure 4a represents the mechanical response (Σ_{11}, E_{11}) in uniaxial tension. The stress distributions in each phase are described for two macroscopic plastic

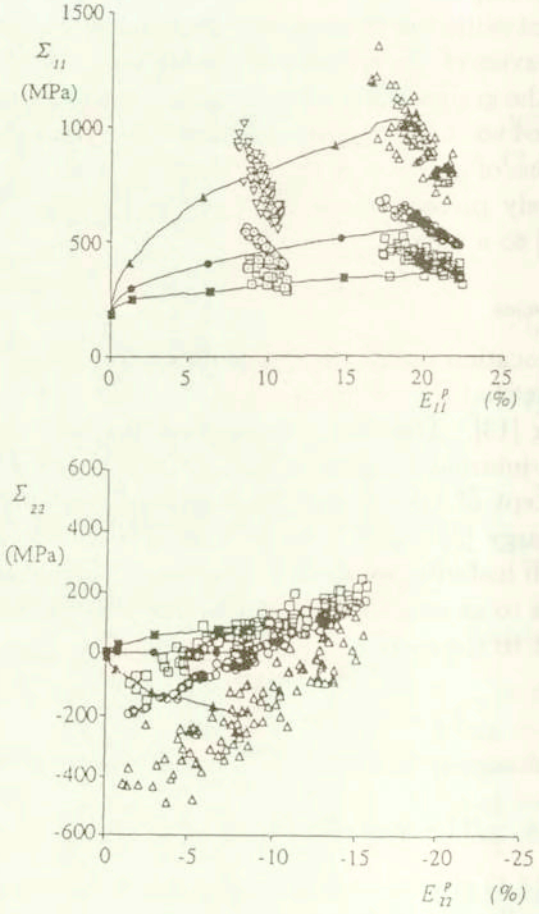

FIG. 4. Mechanical states during an uniaxial tensile test. a) – Macroscopic response of the polycrystal (—●—), mean stresses and strains over the hard phase (—▲—) and soft phase (—■—), mechanical state $(\sigma_{11}, \varepsilon_{11}^P)$ for each grain at: $E_{11}^P = 0.1$ (o) and $E_{11}^P = 0.2$ (o), mechanical state $(\sigma_{11}, \varepsilon_{11}^P)$ for each phase at: $E_{11}^P = 0.1$ (∇, □) and $E_{11}^P = 0.2$ (Δ , □). b) Same as for Fig. 4 a) but for σ_{22} and ε_{22}^P components ($E_{11}^P = 0.2$).

strains 0.1 and 0.2 by clouds of square (s) and triangle (h) points (the third order stresses). The mean stresses in each grain are represented by two clouds of circle points for the same two macroscopic plastic strains. The three curves describe respectively the overall behavior of the polycrystal (first order stresses) and the averaged third order stresses. One finds in the Fig. 4b the same description for the components of the stress tensor. In agreement with experimental measurements by MUGHRABI [35], the cloud of phase (h) is more extented than the cloud of phase (s), and third order internal stresses (inside the hard phase) are twice the overall yield stress for the σ_{11} component. One observes that the fluctuations of components σ_{22} and σ_{33} are more important than those concerning the component σ_{11}.

The corresponding evolution of the cell morphology in each grain is given in Fig. 5 for one grain and Fig. 6 for all the grains. Figure 5 shows the evolution of the two semi-axes ratios of the ellipsoid ($r_1 = a_1/a_2$, $r_2 = a_1/a_3$) during the plastification. After a few percent of plastic strain, a saturation of the cell shape evolution occurs as it was observed on BCC polycrystals by SCHMITT [13]. One can explain this saturation by the stabilisation of the multislip deformation mode. Figure 6 allows to follow the mean evolution of the highest semi-axis ratio of the ellipsoid. Starting from a spherical shape in the reference state, the cells become more and more elongated and reach a stable shape for a few percent of

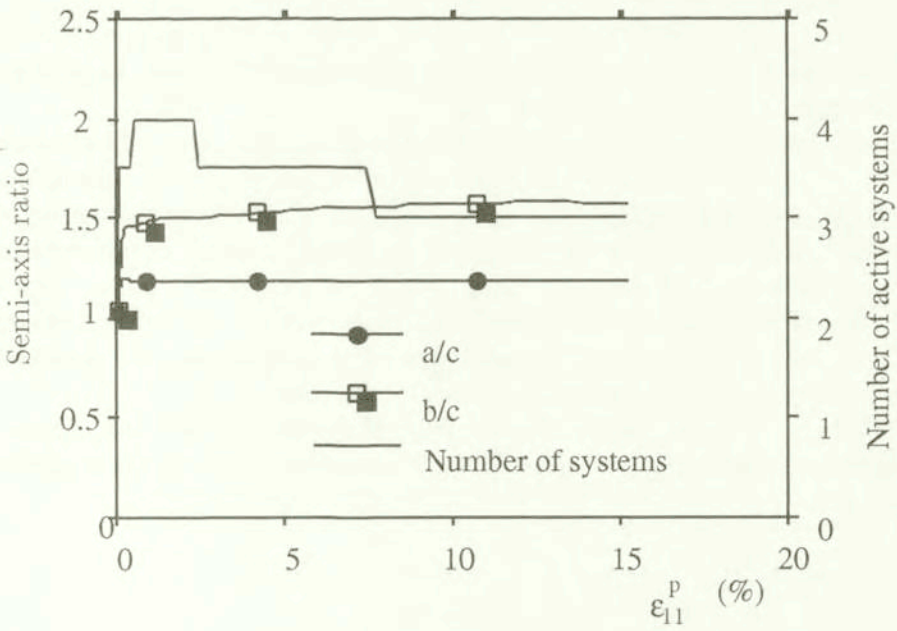

FIG. 5. Evolution of semi-axis ratio in one particular grain of the polycrystal during the loading path.

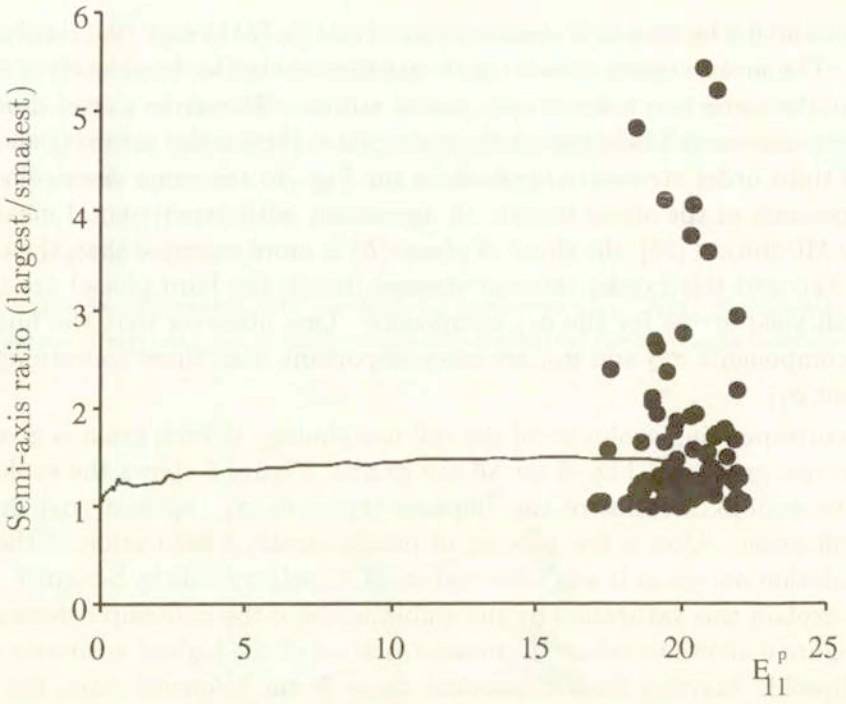

FIG. 6. Evolution of the largest semi-axis ratio in all grains as a function of E_{11}^P.

plastic strain. The cloud of points represents the highest semi-axis ratio in each grain at $E_{11}^P = 0.2$. These remarks (final shape and saturation) have been confirmed experimentally by SCHMITT [13].

In the present applications, the volume fraction f was assumed to be constant so that the results obtained better apply to the formation of stable dislocation cell structures. On the contrary, if the volume fraction is allowed to change, an overall softening is obtained. This softening will be able to produce strain localization as it was shown in [43] and [44]. Thus even if the model is formulated for small elastic-plastic strains, it is well adapted to capture strain localization effect; this is due to the fact that the third order stress fluctuations and the possibility to have a changing microstructure are taken into account.

This way of modelling is different from those used by PIERCE, ASARO and NEEDLEMAN [45] where third order effects are neglected but a large strain formulation is used.

5. Conclusions

Contrary to the grain boundaries, which are stationary with respect to the material, dislocation walls are considered as free surfaces of plastic strain discontinuities similar to a single dislocation which is a linear defect.

Plasticity can be described at various spatial levels. In the common "micro-macro" approach, the local constitutive equations are written in the framework of classical continum mechanics (i. e. with internal variable) and induced dislocation microstructures are not explicity taken into account. The most important physics related with the dislocation walls are the kinematical and the statical boundary conditions which are written here assuming uniform plastic strain inside the cells and the walls. The field fluctuations at the level of the dislocations are lost by the two-phase representation but third order effects (fluctuations at the length scale of cells) are found.

Like in the framework of classical crystal plasticity, some phenomenological parameters and relations describing the hardening and the evolution of the internal state are introduced. Future work has to be done in order to base some phenomenological aspects of the model on a more precise physical description. Applied for complex loading paths, a similar model was able to describe correctly the subsequent behavior [43].

Appendix A

A.1. Interfacial operators [36]

Consider a surface S between two different phases whose plastic strain is denoted by ε^{p1} and ε^{p2}, respectively. The stress and strain tensors are discontinuous across S. HILL [36] has explained how their jumps are related together by interfacial operators. The equilibrum equations:

$$[\sigma_{ij}n_j] = (\sigma^2_{ij} - \sigma^1_{ij})n_j = 0 \tag{A.1}$$

and compatibility conditions:

$$[\varepsilon_{ij}] = \varepsilon^2_{ij} - \varepsilon^1_{ij} = \frac{1}{2}(\lambda_i n_j + \lambda_j n_i), \tag{A.2}$$

where λ_i is a vector determined completely by the condition

$$C_{ijkl}\lambda_k n_l n_j = C_{ijkl}[\varepsilon^p_{kl}]n_j \ , \tag{A.3}$$

lead to the relation:

$$[\varepsilon_{ij}] = P_{ijkl}C_{klmn}[\varepsilon^p_{mn}]. \tag{A.4}$$

P is an interfacial operator depending of the unit normal n_i to the surface S and homogeneous elastic tensor C. The operator P [29] can be written as

$$P_{ijkl} = \frac{1}{4}(C^{-1}_{ik}n_j n_l + C^{-1}_{jl}n_j n_k + C^{-1}_{ik}n_i n_l + C^{-1}_{jl}n_i n_k), \tag{A.5}$$

where C^{-1} denotes the inverse of the Christoffel matrix defined by

$$C_{ik} = C_{ijkl} n_j n_l. \tag{A.6}$$

From (A.3) and (A.4), the stress jump across the surface S is given by

$$[\sigma_{ij}] = -Q_{ijkl}[\varepsilon^p_{kl}], \tag{A.7}$$

where

$$Q_{ijkl} = (I_{ijmn} - C_{ijpq} P_{pqmn}) C_{mnkl}. \tag{A.8}$$

A.2. Determination of the tensor J (Eq. (3.16))

$$J = \int_S Q w_\alpha n_\alpha dS. \tag{A.9}$$

Consider an infinitely extended material with homogeneous elastic tensor C containing an ellipsoidal inclusion V bounded by the surface S. From classical results [37 - 39], the relation between the Green tensor G and the interfacial operator P is given by:

$$\int_V \Gamma(r^+ - r') : C dV' - \int_V \Gamma(r^- - r') : C dV' = P : C \tag{A.10}$$

where

$$\Gamma_{ijkl} = \frac{1}{2}(G_{ik,jl} + G_{jk,il}); \tag{A.11}$$

r' and $r^- \in V$, r^+ is an external point to V and near to S.
Using the definition of the Eshelby tensor [30]

$$S^E = -\int_V \Gamma(r^- - r') : C dV', \tag{A.12}$$

we have

$$\int_V \Gamma(r^+ - r') : C dV' = P : C - S^E. \tag{A.13}$$

On the other hand, the time derivative of S^E (A.12) gives

$$\dot{S}^E = -\int_{S^+} \Gamma(r^- - r^+) : C w_\alpha n_\alpha dS; \tag{A.14}$$

$\dot{S}^E$ is homogeneous inside the ellipsoidal inclusion [40]. Thus, we have

$$\dot{S}^E = \frac{1}{V}\int_V \dot{S}^E dV. \tag{A.15}$$

Applying (A.15) to (A.14) and using (A.13) and the property of Green tensor G

$$\int_V \Gamma(r^- - r'^+)dV' = \int_V \Gamma(r^+ - r'^-)dV', \tag{A.16}$$

we obtain

$$\dot{S}^E v = \int_{S^+} (S^E - P : C)w_\alpha n_\alpha dS. \tag{A.17}$$

By the definition $\dot{V} = \int_{S^+} w_\alpha n_\alpha dS$, we have the integral

$$\int_{S^+} P : C w_\alpha n_\alpha dS = S^E \dot{v} - \dot{S}^E V. \tag{A.18}$$

Using (A.8), the integral J (A.9) is given by

$$J_{ijkl} = C_{ijmn}(I_{mnkl} - S^E_{mnkl})\dot{v} + C_{ijmn}S^2_{mnklpq}\dot{A}_{pq}v \tag{A.19}$$

with $\dot{S}^E = S^2 : \dot{A}$ (see Appendix B).

Appendix B. Determination of the tensors S^E, S^2, and S^3

B.1. Characterization of an ellipsoid and its evolution

The Eshelby tensor S^E is defined by the volume integral (A.12) and its time derivative $\dot{S}^E$ by the surface integral (A.14). Using the divergence theorem, (A.14) becomes:

$$\dot{S}^E = \int_V \Gamma_{,\alpha}(r - r') : C w_\alpha dV' - \int_V \Gamma(r - r')w_{\alpha,\alpha}dV'. \tag{B.1}$$

The time derivative of $\dot{S}^E$ is also given by

$$\text{(B.2)} \qquad \frac{d\dot{S}^E}{dt} = \ddot{S}^E = \int_v \Gamma_{,pq}(r-r') : C w_p w_q dV' - \int_v \Gamma_{,p}(r-r') : C(w_{p,q}w_q + w_p w_{q,q})dV' - \int_v \Gamma_{,q}(r-r') : C w_{p,p} w_q dV' - \int_v \Gamma(r-r') : C(w_{p,pq}w_q + w_{p,p}w_{q,q})dV' - \int_v \Gamma_{,p}(r-r') : C\dot{w}_p dV' - \int_v \Gamma(r-r') : C\dot{w}_{p,p} dV' .$$

The evaluation of these volume integrals requires the knowledge of the velocity w_α and its time and spacial derivatives which can be deduced easily from the kinematical evolution of the ellipsoid v.

Indeed, an ellipsoid is described by semi-axes $a_i (i = 1, 2, 3)$ and Euler angles $\alpha_i (i = 1, 2, 3)$ giving the orientation of the ellipsoid principal reference frame versus the crystalline lattice. These parameters can be regrouped in the tensor $A(a_p, \alpha_p)$ defined by

$$\text{(B.3)} \qquad A_{ij} x_i x_j = 1.$$

In the principal axis of the ellipsoid, A takes the following form:

$$\text{(B.4)} \qquad A^e_{ij} = \begin{pmatrix} 1/a_1^2 & 0 & 0 \\ 0 & 1/a_2^2 & 0 \\ 0 & 0 & 1/a_3^2 \end{pmatrix}.$$

A standard coordinate transformation by the orthogonal matrix $b(\alpha_i)$ gives the tensor A in the crystalline lattice as

$$\text{(B.5)} \qquad A_{ij}(a_k, \alpha_l) = b_{im}(\alpha_l) b_{jn}(\alpha_l) A^e_{mn}(a_k).$$

By time derivative of (B.3), we obtain for w_α:

$$\text{(B.6)} \qquad w_i = \dot{x}_i = -\frac{1}{2} A^{-1}_{ik} \dot{A}_{kl} x_l$$

and its time and spatial derivatives

$$w_{i,j} = \dot{x}_{i,j} = -\frac{1}{2} A^{-1}_{ik} \dot{A}_{kj} , \qquad w_{i,jk} = 0 ,$$

$$\dot{w}_i = \frac{1}{2} \left\{ \frac{3}{2} A^{-1}_{ik} \dot{A}_{kl} A^{-1}_{lm} \dot{A}_{mn} x_n - A^{-1}_{ik} \ddot{A}_{kl} x_l \right\},$$

$$\dot{w}_{i,j} = \frac{1}{2} \left\{ A^{-1}_{im} \dot{A}_{mn} A^{-1}_{nk} \dot{A}_{kj} - A^{-1}_{ik} \ddot{A}_{kj} \right\} .$$

For the application of the consistency relation, a second derivative of S^E is also needed so that we have to determine

$$\dot{S}^E_{ijkl} = S^2_{ijklpq}\dot{A}_{pq}\,, \qquad \ddot{S}^E_{ijkl} = S^3_{ijklpqrs}\dot{A}_{pq}\dot{A}_{rs} + S^2_{ijklpq}\ddot{A}_{pq}, \tag{B.8}$$

where the new tensors S^2 and S^3 are defined from to S^E by

$$S^2_{ijklpq} = \frac{\partial S^E_{ijkl}}{\partial A_{pq}}\,, \qquad S^3_{ijklpqrs} = \frac{\partial^2 S^E_{ijkl}}{\partial A_{pq}\partial A_{rs}} \tag{B.9}$$

and given by the following expressions:

$$S^2_{ijklpq} = \frac{1}{2}\left(\overline{S}^2_{ijklpq} + \overline{S}^2_{ijklpqrs}\right)\,, \qquad S^3_{ijklpqrs} = \frac{1}{2}\left(\overline{S}^3_{ijklpqrs} + \overline{S}^3_{ijklpqrs}\right)\,,$$

$$S^E_{ijkl} = \frac{1}{2}\left(\overline{S}^E_{ijkl} + \overline{S}^E_{ijkl}\right) \tag{B.10}$$

with

$$\begin{aligned}
\overline{S}^2_{ijklpq} &= -\frac{1}{4}\left\{T^2_{ijmntp}A^{-1}_{tq} + T^2_{ijmntq}A^{-1}_{tp} - 2T^1_{ijmn}A^{-1}_{pq}\right\}C_{mnkl}\,,\\
\overline{S}^3_{ijklpqrs} &= -\frac{1}{16}\left\{T^3_{ijmntqus}A^{-1}_{tp}A^{-1}_{ur} + T^3_{ijmntpus}A^{-1}_{tq}A^{-1}_{ur}\right.\\
&\qquad \left. + T^3_{ijmntqur}A^{-1}_{tp}A^{-1}_{us} + T^3_{ijmntpur}A^{-1}_{tq}A^{-1}_{us}\right\}C_{mnkl}\\
&\quad + \frac{1}{8}\left\{T^2_{ijmnts}(A^{-1}_{tp}A^{-1}_{qr} + A^{-1}_{tq}A^{-1}_{pr} + A^{-1}_{pq}A^{-1}_{tr}) + T^2_{ijmntr}(A^{-1}_{tp}A^{-1}_{qs}\right.\\
&\quad + A^{-1}_{tq}A^{-1}_{ps} + A^{-1}_{pq}A^{-1}_{ts}) + T^2_{ijmntq}(A^{-1}_{tr}A^{-1}_{sp} + A^{-1}_{ts}A^{-1}_{rp} + A^{-1}_{rs}A^{-1}_{tp})\\
&\qquad \left. + T^2_{ijmntp}(A^{-1}_{tr}A^{-1}_{sq} + A^{-1}_{ts}A^{-1}_{rq} + A^{-1}_{rs}A^{-1}_{tq})\right\}C_{mnkl}\\
&\qquad - \frac{1}{4}T^1_{ijmn}C_{mnkl}\left(A^{-1}_{pq}A^{-1}_{rs} + A^{-1}_{rp}A^{-1}_{qs} + A^{-1}_{rq}A^{-1}_{ps}\right),\\
\overline{S}^E_{ijkl} &= T^1_{ijmn}C_{mnkl}.
\end{aligned}$$

The tensors T^1, T^2 and T^3 are given in the condensed form:

$$\mathcal{T}_{ijkl} = -\frac{D\partial^2}{\partial x_j \partial x_l}\int G_{ik}(r - r')f(r')dV'\,, \tag{B.11}$$

where D denotes a differential operator and $f(r')$ is a function such that three choices are possible:

$$\text{(B.12)} \quad \begin{aligned} &D = 1\,, && f(r') = 1 && \forall r' \in v \text{ then } \mathcal{T} = T^1;\\ &D = \frac{\partial}{\partial x_m}, && f(r') = x'_n && \forall r' \in v \text{ then } \mathcal{T} = T^2\,;\\ &D = \frac{\partial^2}{\partial x_m \partial x_p}, && f(r') = x'_n x'_q && \forall r' \in v \text{ then } \mathcal{T} = T^3. \end{aligned}$$

The tensor $\mathcal{T}$ (B.11) can be calculated using Fourier's transformation of the Green tensor G.

B.2. Numerical method by Fourier transformation

The explicit calculation of the Green tensor G from the equation

$$\text{(B.13)} \qquad C_{ijkl} G_{jn,ik}(r) + \delta_{ln}\delta(r) = 0$$

can be accomplished by Fourier's transformation. $\delta(r)$ and δ_{ln} are respectively the distribution of Dirac and Kronecker's symbol. If $\tilde{G}(k)$represents the Fourier transformation of $G(r)$, then

$$\text{(B.14)} \qquad \tilde{G}(k) = \int_v G(r) e^{-ik_s x_s} dV, \quad G(r) = \frac{1}{8\pi^3} \int_{v_k} \tilde{G}(k) e^{ik_s x_s} dV_k$$

so that the transform of (B.13) is

$$\text{(B.15)} \qquad C_{ijkl} \tilde{G}_{jk} k_i k_k = \delta_{ln}.$$

The vector k may be described with the spherical coordinates $\mathbf{k}$, θ, φ by

$$\text{(B.16)} \qquad k_j = \mathbf{k} X_j, \qquad (j = 1, 2, 3),$$

where

$$\text{(B.17)} \qquad X_1 = \sin\theta\cos\varphi, \quad X_2 = \sin\theta\sin\varphi, \quad X_3 = \cos\theta,$$

with $\mathbf{k} \in [0, +\infty]$, $\theta \in [0, \pi]$, $\varphi \in [0, 2\pi]$.
Consequently (B.15) becomes

$$\text{(B.18)} \qquad \mathbf{k}^2 \tilde{G}_{jn}(k) = M^{-1}_{jn}(X),$$

where the matrix M depends on the orientation of the vector k by

$$\text{(B.19)} \qquad M_{jn}(X) = C_{jknl} X_k X_l.$$

Integration with respect to k in (B.14) uses spherical layers $S(X)$ of thickness $d\mathbf{k}$ and mean radius $\mathbf{k}$, and it gives:

$$dV_k = \mathbf{k}^2 d\mathbf{k} dS(X) \quad \text{with} \quad dS(X) = \sin\theta d\theta d\varphi, \tag{B.20}$$

so that with these equations, (B.11) becomes

$$\mathcal{T}_{ijkl} = -\frac{1}{8\pi^3} \frac{D\partial^2}{\partial x_j \partial x_l} \int_S M_{ik}^{-1}(X) dS \int_V f(r') \int_0^\infty e^{i\mathbf{k}X_s(x_s - x_s')} d\mathbf{k} dV'. \tag{B.21}$$

Following FAIVRE [41], only the real part of the integral of $e^{i\mathbf{k}X_s(x_s - x_s')}$ gives a non-zero contribution,

$$Re \int_0^\infty e^{i\mathbf{k}X_s(x_s - x_s')} d\mathbf{k} = \frac{1}{2} \int_{-\infty}^{+\infty} e^{i\mathbf{k}X_s(x_s - x_s')} d\mathbf{k},$$

but in terms of the unidimensional Dirac function δ, we have

$$\int_{-\infty}^{+\infty} e^{i\mathbf{k}\eta} d\mathbf{k} = 2\pi\delta(\eta).$$

Finally (B.21) is rewritten as

$$\mathcal{T}_{ijkl} = -\frac{1}{8\pi^2} \int_S M_{ik}^{-1}(X) \frac{D\partial^2}{\partial x_j \partial x_l} \int_V f(r')\delta(X_s(x_s - x_s')) dV' dS. \tag{B.22}$$

Recalling that function f is zero outside the ellipsoid V, we can extend the integral $\int_v f(r')\delta(X_s(x_s - x_s))dV'$ over the infinite volume. Then, observing that equation

$$\mathbf{X}(\mathbf{r} - \mathbf{r}') = 0$$

represents a plane $\mathcal{P}(\mathbf{r}')$ passing throught point r and with unit normal X, we obtain the case of the Dirac function concentrated on plane $\mathcal{P}(\mathbf{r}')$. Using KECS and TEODORESCU [42], we have:

$$I_f(r) = \int_{-\infty}^{+\infty} f(r')\delta(X_m(x_m - x_m'))dV' = \frac{1}{\chi_\alpha} \int_p f(r')dx_r' dx_s \tag{B.23}$$

with (α, r, s) being equal to any permutation of $(1, 2, 3)$.

$I_f(r)$ is a classical surface integral that gives for a point r **located in the ellipsoid** the following three results:

- first case of (B.12): $f(r') = 1$ then $I_f(r) = \dfrac{a_1 a_2 a_3 \pi}{Z}(1 - H^2)$

with $Z = \sqrt{a_1^2 X_1^2 + a_2^2 X_2^2 + a_3^2 X_3^2}$, $H = \dfrac{X_i x_i}{Z}$;

- second case of (B.12): $f(r') = x_n$ then $I_f(r) =$

$$= a_N^2 X_n \frac{a_1 a_2 a_3 \pi}{Z^2}(1 - H^2)H;$$

- third case of (B.12): $f(r') = x_n x_q$ then $I_f(r) =$

$$= a_N^2 a_Q^2 X_n X_q \frac{a_1 a_2 a_3 \pi}{Z^3}(1 - H^2)H^2.$$

Substituting the three possible choices into (B.22), we obtain by performing the partial differentiations D, $\dfrac{\partial}{\partial x_j}$ and $\dfrac{\partial}{\partial x_l}$:

$$T^1_{ijkl} = \frac{a_1 a_2 a_3}{4\pi} \int_\Omega M^{-1}_{ik}(X) \frac{X_j X_l}{k^3} d\Omega,$$

$$T^2_{ijklmn} = \frac{3 a_1 a_2 a_3 a_N^2}{4\pi} \int_\Omega M^{-1}_{ik}(X) \frac{X_j X_l X_m X_n}{k^5} d\Omega, \tag{B.24}$$

$$T^3_{ijklmnpq} = \frac{3 a_1 a_2 a_3 a_N^2}{\pi} \int_\Omega M^{-1}_{ik}(X) \frac{X_j X_l X_m X_n X_p X_q}{k^5} d\Omega.$$

Let us observe that T^1, T^2 and T^3 do not depend on r for r lying inside the ellipsoid; this result was previously mentioned by Eshelby for T^1.

Calculations of these tensors require the knowledge of M_{ik} given from (B.21): in the general case of an ellipsoidal inclusion and anisotropic material, a numerical method is used. In the next section the case of spherical inclusion and isotropic material is solved analytically.

B.3. Isotropic elasticity – flattening of a sphere into ellipsoid

From the components M_{ik} (B.19) we obtain for isotropic elasticity with shear modulus μ and Poisson's ratio v the result:

$$M^{-1}_{ik}(X) = \frac{1}{\mu}(\delta_{ik} - \frac{1}{2(1-v)} X_i X_k). \tag{B.25}$$

Substituting for a sphere $a_1 = a_2 = a_3$ and (B.25) in (B.24), we obtain tensors T^1, T^2 and T^3:

$$T^1_{ijkl} = \frac{1}{30(1-v)\mu}\left((9 - 10v)\delta_{ik}\delta_{jl} - (\delta_{ij}\delta_{kl} + \delta_{il}\delta_{jk})\right),$$

$$T^2_{ijklmn} = \frac{1}{70(1-v)\mu}\Big((13-14v)\delta_{ik}(\delta_{jl}\delta_{mn} + 2\overline{\Delta}_{jlmn}) - \delta_{ij}\delta_{kl}\delta_{mn}$$
$$-\delta_{il}\delta_{jk}\delta_{mn} - 2\delta_{ij}\overline{\Delta}_{klmn} - 2\delta_{kl}\overline{\Delta}_{ijmn} - 2\delta_{il}\overline{\Delta}_{jkmn} - 2\delta_{im}\overline{\Delta}_{jnkl}$$
$$-2\delta_{in}\overline{\Delta}_{jmkl}\Big),$$

$$T^3_{ijklmnpq} = \frac{2}{315(1-v)\mu}\Big((17-18v)\delta_{ik}(\delta_{jl}\delta_{mn}\delta_{pq} + 2\delta_{jl}\overline{\Delta}_{mnpq}$$
$$+2\delta_{pq}\overline{\Delta}_{jlmn} + 2\delta_{mn}\overline{\Delta}_{jlpq} + 8\overline{\Delta}_{jlmnpq}) - (\delta_{ij}\delta_{kl}\delta_{mn}\delta_{pq} + \delta_{il}\delta_{jk}\delta_{mn}\delta_{pq}$$
$$+2\delta_{ij}\delta_{kl}\overline{\Delta}_{mnpq} + 2\delta_{ij}\delta_{mn}\overline{\Delta}_{klpq} + 2\delta_{ij}\delta_{pq}\overline{\Delta}_{klmn} + 2\delta_{kl}\delta_{mn}\overline{\Delta}_{ijpq}$$
$$+2\delta_{kl}\delta_{pq}\overline{\Delta}_{ijmn} + 2\delta_{il}\delta_{mn}\overline{\Delta}_{jkpq} + 2\delta_{ip}\delta_{mn}\overline{\Delta}_{jqkl} + 2\delta_{iq}\delta_{mn}\overline{\Delta}_{jpkl}$$
$$+2\delta_{il}\delta_{pq}\overline{\Delta}_{jkmn} + 2\delta_{im}\delta_{pq}\overline{\Delta}_{jnkl} + 2\delta_{in}\delta_{pq}\overline{\Delta}_{jmkl} + 2\delta_{il}\delta_{jk}\overline{\Delta}_{mnpq}$$
$$+8\delta_{ij}\overline{\overline{\Delta}}_{klmnpq} + 8\delta_{kl}\overline{\overline{\Delta}}_{ijmnpq} + 8\delta_{il}\overline{\Delta}_{jkmnpq} + 16\overline{\overline{\nabla}}_{ijmnklpq}$$
$$+16\overline{\overline{\nabla}}_{ijpqklmn} + 4\overline{\Delta}_{ijmn}\overline{\Delta}_{klpq} + 4\overline{\Delta}_{ijpq}\overline{\Delta}_{klmn})\Big),$$

with

$$\overline{\Delta}_{ijkl} = \frac{1}{2}(\delta_{ik}\delta_{jl} + \delta_{il}\delta_{jk}),$$

$$\overline{\overline{\Delta}}_{ijklmn} = \frac{1}{4}(\delta_{ik}\overline{\Delta}_{jlmn} + \delta_{il}\overline{\Delta}_{jkmn} + \delta_{im}\overline{\Delta}_{jnkl} + \delta_{in}\overline{\Delta}_{jmkl}),$$

$$\overline{\overline{\nabla}}_{ijklmnpq} = \frac{1}{2}(\delta_{ik}\overline{\overline{\Delta}}_{jlmnpq} + \delta_{il}\overline{\overline{\Delta}}_{jkmnpq}).$$

References

1. G.Y. TAYLOR, *Plastic strain in metals*, J. Inst. Metals., **62**, 307, 1938.
2. G. SACHS, *Zur Ableitung einer Fliessbedingung*, Z. der V.D.I., **72**, 739, 1928.
3. M. BERVEILLER and A. ZAOUI, *Méthodes self-consistentes en mécanique des solides hétérogenes*, Comportements rhéologiques et structures des matériaux, C. HUET and A. ZAOUI [Eds.], 175, 1981.
4. P. LIPINSKI and M. BERVEILLER, *Elastoplasticity of microinhomogeneous metals at large strains*, Int. J. of Plast., **5**, 149, 1989.
5. P. LIPINSKI, J. KRIER and M. BERVEILLER, *Elastoplasticité des métaux en grandes déformations: comportement global et évolution de la structure interne*, Rev. Phys. Appl., **25**, 361, 1990.
6. P. LIPINSKI, M. BERVEILLER, E. REUBREZ and J. MORREALE, *Transition theories of elastic-plastic deformation of metallic polycrystals*, Arch. of Appl. Mech., **95**, 291, 1995.
7. Z. HU, E.F. RAUCH and C. TEODOSIU, *Work-hardening behavior of mild steel under stress reversal at large strains*, Int. J. Plast., **7**, 839, 1992.

8. C. REY, *Effects of grain boundaries on the mechanical behavior of grains in polycrystals*, Revue Phys. Appl., **23**, 491, 1988.

9. A. KORBEL and P. MARTIN, *Microscopic versus macroscopic aspect of shear bands deformation*, Acta Met., **34**, 1905, 1986.

10. S. THUILLIER, *Rhéologie et microstructure associées á un trajet complexe de déformation pour une nuance d'acier doux*, Thése de INPG Grenoble 1992.

11. U. ESSMANN and H. MUGHRABI, *Annihilation of dislocations during tensile and cyclic deformation and limits of dislocation densities*, Phil. Mag., A **40**, 735, 1979.

12. A. LUFT, *Microstructural processes of plastic instabilities in strengthened metals*, Prog. Mater. Sci., **35**, 97, 1991.

13. J. H. SCHMITT, *Contribution á l'étude de la micro-plasticité des aciers*, Thése de INPG Grenoble 1986.

14. X. LEMOINE, D. MULLER and M. BERVEILLER, *Texture of microstructures in BCC metals for various loading paths*, Mat. Science Forum **157–162**, 1821, 1994.

15. D. MULLER, X. LEMOINE and M. BERVEILLER, *Nonlocal behavior of elastoplastic metals : theory and results*, Trans. of the ASME, **116**, 378, 1994.

16. F. B. PRINZ and A. S. ARGON, *Dislocation cell formation during plastic deformation of copper single crystals*, Phys. Stat. Sol., **57**, 741, 1980.

17. L. P. KUBIN and Y. ESTRIN, *Strain nonuniformities and plastic instabilities*, Revue Phys. Appl., **23**, 573, 1988.

18. S. B. GORYACHEV and A. V. SHALENKOV, *Theory and computer simulation of dislocation structure relaxation during annealing*, Solid State Phenomena, **35–36**, 375, 1994.

19. E. C. AIFANTIS, *Higher order gradients and self-organization at nano, micro and macro-scales*, Mat. Science Forum CMDS7, 55, 1993.

20. J. KRATOCHVIL, *Continuum mechanics approach to collective behavior of dislocations*, Solid State Phenomena, **35–36**, 71, 1994.

21. A. FENNAN, *Homogénéisation élastoplastique discréte*, Thèse de l'Ecole Centrale de Lyon 1995.

22. D. KUHLMANN-WILSDORF, LEDS, *Properties and effects of low energy dislocation structure*, Mater. Sci. and Engng., **86**, 53, 1987.

23. D. KUHLMANN-WILSDORF, *Theory of plastic deformation: properties of low energy dislocation structure*, Mater. Sci. and Engng., **A113**, 1, 1989.

24. P. GERMAIN, *Cours de mécanique des milieux continus*, Théorie générale, eds. Masson et Cie, Paris **1**, 1973.

25. J. R. RICE, *Inelastic constitutive relations for solids : an internal-variable theory and its application to metal plasticity*, J. Mech. Phys. Solids, **19**, 433, 1971.

26. G. A. MAUGIN, *The thermodynamics of plasticity and fracture*, Cambridge in Applied mathematics, eds. Cambridge University Press 1992.

27. J. HADAMARD, *Leçons sur la propagation des ondes et les équations de l'hydrodynamique*, Cours du Collége de France, Paris 1903.

28. H. INAGAKI, *Development of microstructures and textures during cold rolling of polycrystalline iron containing an excess amount of dissolved carbon*, Z. Metalkde, 474, 1989.

29. R. HILL, *Interfacial operators in the mechanics of composite media*, J. Mech. Phys. Solids, **31**, 347, 1983.

30. J. D. ESHELBY, *The determination of the elastic field of an ellipsoidal inclusion and related problems*, Proc. Roy. Soc., **A241**, 376, 1957.

31. E. KRÖNER, *Zur plastischen Verformung des Vielkristalls*, Acta Metall., **9**, 155, 1961.

32. D. MULLER, J. KRATOCHVIL and M. BERVEILLER, *Effets des écrouissages couplés de différentes parties d'un métal sur la réponse en traction-compression et sur les contraintes internes*, C. R. Acad. Sci., **316**, 435, 1993.

33. D. MULLER, *Influence de l'écrouissage non local et de l'hétérogénéisation intragranulaire sur le comportement des aciers polycristallins*, Thèse, Université de Metz 1994.

34. P. FRANCIOSI, M. BERVEILLER and A. ZAOUI, *Latent hardening in copper and aluminium single crystal*, Acta Met., **28**, 273, 1980.

35. H. MUGHRABI, *Dislocation clustering and long-range internal stresses in monotically and cyclically deformed metal crystals*, Revue Phys. Appl., **23**, 367, 1988.

36. R. HILL, *An invariant treatment of interfacial discontinuities in elastic composites*, Continuum Mechanics and Related Problems of Analysis, 597, Moscow 1972.

37. M. CHERKAOUI, H. SABAR and M. BERVEILLER, *Micromechanical approach of the coated inclusion problem and applications to composite materials*, Trans. of the ASME, **16**, 274, 1994.

38. M. CHERKAOUI, H. SABAR and M. BERVEILLER, *Elastic composites with coated reinforcements : a micromechanical approach for non homothetic topology*, Int. J. Engng Sci., **33**, 829, 1995.

39. L. J. WALPOLE, *A rotated rigid ellipsoidal inclusion in an elastic medium*, Proc. R. Soc. Lond. **A 433**, 179, 1991.

40. H. SABAR, M. BUISSON and M. BERVEILLER, *The inhomogeneous and plastic inclusion problem with moving boundary*, Int. J. Plast., **7**, 759, 1991.

41. G. FAIVRE, *Hétérogénéités ellipsoidales dans un milieu élastique anisotrope*, J. Physique, **32**, 325, 1971.

42. W. KECS and P. P. TEODORESCU, *Applications of the theory of distributions in mechanics*, Abacus Press, England 1974.

43. I. AUBERT, *Effet de l'hétérogénéisation plastique sur le comportement macroscopique lors de chargements complexes*, Thèse de l'Université de Metz, 1998.

44. M. BERVEILLER, M. CHERKAOUI and I. AUBERT, *Micromechanics of moving inelastic discontinuities and applications*, Proceeding of the IUTAM Symposium Micro and Macrostructural Aspects of Thermoplasticity, Bochum, Germany, 25–29 August 1997.

45. D. PIERCE, R. J. ASARO and NEEDLEMAN, *Material rate-dependence and localized deformation in crystalline solids*, Acta Metall., **31**, 12, pp. 1951–1976, 1983.

LABORATOIRE DE PHYSIQUE ET MECANIQUE DES MATERIAUX
INSTITUT SUPERIEUR DE GENIE MECANIQUE ET PRODUCTIQUE
Metz, France
and
LABORATOIRE D'ETUDES ET DE DEVELOPPEMENT DES PRODUITS PLATS
Sollac, Florange, France

Received December 9, 1997